IOPscience iopscience.iop.org

Home Search Collections Journals About Contact us My IOPscience

Strong excitons in novel two-dimensional crystals: Silicane and germanane

This content has been downloaded from IOPscience. Please scroll down to see the full text.

2012 EPL 98 37004

(http://iopscience.iop.org/0295-5075/98/3/37004)

View the table of contents for this issue, or go to the journal homepage for more

Download details:

IP Address: 128.148.252.35
This content was downloaded on 29/09/2013 at 07:14

Please note that terms and conditions apply.

A Letters Journal Exploring the Frontiers of Physics

May 2012

EPL, **98** (2012) 37004
doi: 10.1209/0295-5075/98/37004

www.epljournal.org

Strong excitons in novel two-dimensional crystals: Silicane and germanane

O. Pulci[1,2,4], P. Gori[2,4], M. Marsili[1,4], V. Garbuio[1,4], R. Del Sole[1,4] and F. Bechstedt[3,4]

[1] *Dipartimento di Fisica, Università di Roma Tor Vergata - Via della Ricerca Scientifica 1, I-00133 Rome, Italy, EU*
[2] *CNR-ISM - Via Fosso del Cavaliere 100, I-00133 Rome, Italy, EU*
[3] *IFTO, Friedrich Schiller Universität - Max-Wien Platz 1, D-07742 Jena, Germany, EU*
[4] *European Theoretical Spectroscopy Facility*

received 5 February 2012; accepted 10 April 2012
published online 11 May 2012

PACS 71.35.Cc – Intrinsic properties of excitons; optical absorption spectra
PACS 73.22.-f – Electronic structure of nanoscale materials and related systems
PACS 78.67.Wj – Optical properties of graphene

Abstract – We show by first-principles calculations that, due to depressed screening and enhanced two-dimensional confinement, excitonic resonances with giant oscillator strength appear in hydrogenated Si and Ge layers, which qualitatively and quantitatively differ from those of graphane. Their large exciton binding energies and oscillator strengths make them promising for observation of novel physical effects and application in optoelectronic devices on the nanoscale.

Copyright © EPLA, 2012

Introduction. – The realization of graphene, the two-dimensional (2D) sp^2-bonded form of carbon (C), and of its derivatives has led to a revolution in the fields of condensed-matter physics, basic science, and device technology [1,2]. The understanding and control of their properties are continuously leading to novel effects and device proposals [3]. Structural modifications such as in ribbons and chemical treatments by oxygen, hydrogen (H) and doping, make the 2D carbon an ideal material for future nanotechnology [3,4]. For instance, the fully hydrogenated and hence sp^3-bonded graphene, the so-called graphane [4–6], opens the fundamental gap at least up to 5.4 eV [7–9]. At the corresponding absorption edge strongly bound charge transfer excitons occur which may open the way towards the observation of an excitonic Bose-Einstein condensate [10,11]. The progress in the study of the outstanding properties of graphene and its derivatives has generated much interest for its hypothetical silicon (Si) or germanium (Ge) counterparts, silicene and germanene [12,13]. Theoretical studies predict free-standing silicon with similar electronic properties as graphene [13,14], such as the formation of Dirac cones at the Brillouin zone (BZ) corners. The existence of atomic layers of sp^2-bonded Si atoms is still a matter of controversy (see, *e.g.*, [15]). The puckered geometry predicted for the free-standing Si and Ge layers [16], consequence of a mixed sp^2-sp^3 hybridization, proves indeed the resistance of such elements against a pure sp^2 hybridization. Recently, silicene nanoribbons have been observed by scanning tunneling microscopy (STM) and angle-resolved photoemission spectroscopy (ARPES) [17]. In correspondence with the hydrogenation of graphene to graphane (C_2H_2), a new class of 2D or sheet crystals, including also silicane (Si_2H_2) and germanane (Ge_2H_2), comes into the focus.

Interestingly, such H-saturated Si and Ge sheets have been synthesized a long time ago in the form of layered polysilane [18,19] or layered polygermyne [20] and have also been investigated [21]. The properties of the individual sheets are however little known. Only their electronic band structures have been calculated at the density-functional theory (DFT) [22,23] and GW [24] level. The direct band gaps and the strong ultraviolet luminescence of the corresponding Si and Ge polymers [25–27] clearly indicate that the limitations of the indirect semiconductors Si and Ge for optoelectronic applications can be overcome by nanostructuring. However, how the transition from massless to massive Dirac fermions influences the optical properties of the 2D materials graphane, silicane, and germanane is not understood. How the interplay of low dimensionality, extreme carrier localization, modified Coulomb attraction of electrons and holes, as well as reduced screening, influences the formation of excitons has not been investigated. The hydrogenated group-IV sheet crystals represent ideal model system for such studies.

The optical properties of the 2D materials graphane, silicane, and germanane could be very appealing due to the extreme system anisotropy and the electron-hole

Table 1: Ground-state geometry parameters (lattice constant a, characteristic bond length IV-IV and IV-H, sheet buckling) compared with previous theoretical and experimental results. All lengths are in Å.

Sheet	Structural parameter	This work	Other works (Theory)	Other works (Exp)
C_2H_2				
	a	2.54	2.45 [22,33]	2.42[6]
	C-C	1.54	1.49–1.53 [4,7,22,33]	
	C-H	1.11	1.08–1.12 [4,7,22,33]	
	Buckling	0.46	0.45 [22,33]	
Si_2H_2				
	a	3.89	2.82–3.97 [22–24,32,34]	3.8–4.1 [18,35,36]
	Si-Si	2.36	2.32–2.39 [22,23,32,34]	2.35 [19]
	Si-H	1.50	1.50–1.52 [22,23,32,34]	1.15 [19]
	Buckling	0.72	0.69–0.72 [22,23,34]	
Ge_2H_2				
	a	3.95	3.93–4.09 [23,24,32]	3.98 [20]
	Ge-Ge	2.39	0.34–2.47 [22,23,32]	
	Ge-H	1.54	2.54 [32], 1.56[23]	
	Buckling	0.73	1.7 [22], 0.73[23]	

localization in one direction. First-principles calculations of the electronic structures and optical spectra of these materials can help in understanding their properties in their ideal free-standing geometries as well as the chemical trend with the group-IV atoms C, Si or Ge.

In this work, electronic and optical properties of silicane and germanane are studied in the framework of the many-body perturbation theory, and compared with those of graphane.

Methods. – We apply a three-step procedure: i) the equilibrium atomic coordinates and the electronic ground state are obtained using DFT [28][1] ii) the quasiparticle (QP) bands are calculated within Hedin's GW approximation [29,30]; iii) finally, we solve the Bethe-Salpeter equation (BSE) including the screened Coulomb interaction and the unscreened electron-hole exchange for all quasiparticle bands to account for the excitonic effects in the optical spectra [30,31].

Results. – The ground-state geometries (see footnote [1]) of graphane, silicane and germanane, reported in table 1, are in agreement with other DFT calculations [4,7,22,23,32–34], and with the available experimental data [6,18–20,35,36].

Whereas graphene has a flat geometry, its Si and Ge counterparts present a puckered geometry [16]. Upon hydrogenation and the consequent sp^3 hybridization, buckling appears in C_2H_2 (0.46 Å) and is further enhanced in Si_2H_2, and Ge_2H_2, going from 0.44 Å to 0.72 Å in silicane and from 0.63 Å to 0.73 Å in germanane.

[1]The DFT calculations have been performed using a semilocal PBE treatment of exchange and correlation, a plane-wave expansion with a kinetic-energy cutoff of 60 Ry(C_2H_2), 35 Ry(Si_2H_2) and 40 Ry (Ge_2H_2) and a vacuum thickness between the sheets of 43.2 a.u., 36.8 a.u., and 22.4 a.u., respectively.

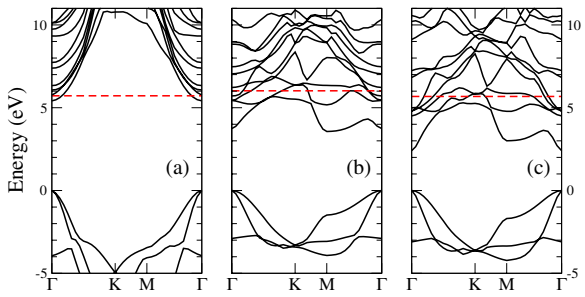

Fig. 1: (Color online) Quasiparticle band structures of graphane (a), silicane (b), and germanane (c). The horizontal red dashed line indicates the vacuum level.

Electronic band structures. The QP band structures, based on fully relaxed atomic geometries, are depicted in fig. 1. They are completely different from the band structures of the non-hydrogenated almost sp^2-bonded group-IV sheets: already at the DFT level the sp^3-coordinated group-IV sheets are insulators with remarkably large gaps at the BZ center Γ [4,10,22]. Once many-body effects are included, the opening of the gaps is sizeable (more than 50%). Indeed, the quasiparticle renormalization effects are enhanced in the atomic-layer systems due to the low dimensionality confirming for silicane and germanane what was shown for graphane [10]. Thereby the positions of the band extrema are far away from the Dirac K and K' points due to hydrogen passivation of the crystal. Germanane shows a direct gap at Γ, while silicane exhibits an indirect gap at $\Gamma \to M$ which however is extremely close to the direct $\Gamma \to \Gamma$ one. The values of the QP gaps are 5.4(C_2H_2), 3.6(Si_2H_2), and 2.4(Ge_2H_2) eV.

The quasiparticle renormalization significantly modifies the electron removal and addition. The absolute position of the lowest empty state in fig. 1 determines the electron

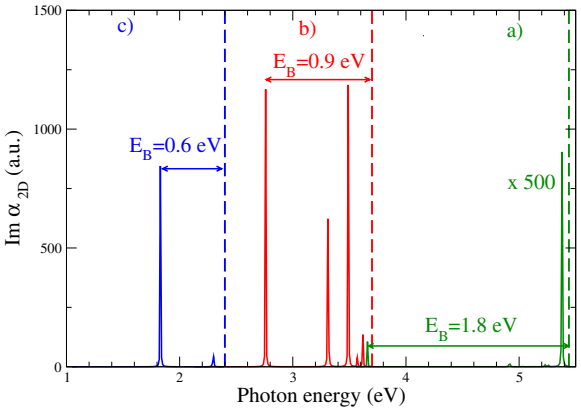

Fig. 2: (Color online) Imaginary part of the macroscopic polarizability $\alpha_{2D} = (\epsilon - 1)L/4\pi$ below the fundamental gap, for light polarization parallel to the sheet. Green: graphane (a); red: silicane (b); black: germanane (c). The vertical dashed lines indicate the lowest direct QP gap.

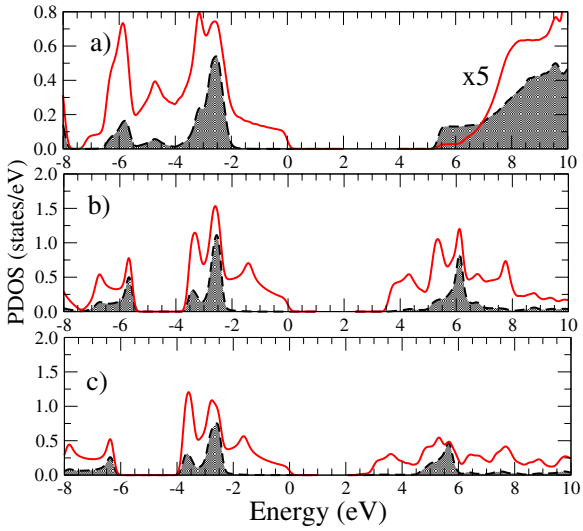

Fig. 3: (Color online) Atom-projected density of states for graphane (a), silicane (b), and germanane (c) around the fundamental quasiparticle gap. The solid red line describes the projections onto group-IV atoms while the black dashed line indicates the H contributions. Conduction states for graphane have been multiplied by a factor 5.

affinity A. For graphene we find a dramatic change of the electron affinity upon hydrogenation, from $A = 4.2\,\mathrm{eV}$ (graphene) to the value $A = 0.3\,\mathrm{eV}$ (graphane) in agreement with Cudazzo *et al.* [10]. The positive value of A is somewhat in contrast to the negative electron affinity of some hydrogenated diamond surfaces (see for example [37] and references therein). This is due to the presence of compensating group-IV–H dipoles on the top and bottom of the sheet. For silicane and germanane A is much larger: $A = 2.5\,\mathrm{eV}$ (4.6 eV in silicene) and 3.3 eV (4.7 eV in germanene), respectively, as for a conventional insulator or semiconductor. The varying values of A for the three materials is mainly a consequence of the different electronegativity of C, Si and Ge with respect to H: while C is more electronegative than H, the opposite holds for Si and Ge. This fact has direct influence also on the character of the indirect/direct gap transition upon dimensionality lowering. For germanane and silicane the transition is due to quantum-confinement effects that shift upward the lowest bulk-unoccupied state (at L, X, respectively), responsible for the bulk indirect gap, while leaving almost unchanged the energy of the lowest unoccupied state at the Γ-point. On the contrary, in the case of graphane the presence of H causes the formation of nearly free electron states near the bottom of the conduction band at the Γ-point [9].

Optical properties. The optical absorption spectra (fig. 2) show an enhanced influence of excitonic effects in the 2D crystals. For all the materials we find a series of bound exciton states with varying spectral strengths below the fundamental quasiparticle gap which move the absorption edge from the UV to the near UV or even visible spectral range. The number of bright bound states varies due to the strength of the electron-hole interaction and to the values of electron and hole effective masses. Analysing the excitonic bound states, we find that the main band contributions are due to electron-hole pairs close to the Γ-point, and that, within each electron-hole pair, the holes are located in the two uppermost valence bands (degenerate at Γ) while the electrons are in the lowest conduction band. Consequently, all excitons are twofold degenerate.

The dominance of the two lowest non-Coulomb-correlated electron-hole band pairs in all bound excitons and the varying binding energy suggest that the bound excitons belong to an exciton series. However, fig. 2 exhibits an apparently odd chemical trend in the average peak strengths of the bound excitons. The average oscillator strengths of the bound states are comparable in germanane and silicane but about 500 times larger than in graphane. This trend, already visible from the absorption edge without excitonic effects (not shown), does not follow the ratio of the squared lattice constants, as it would be expected from the fact that the optical oscillator strength is inversely proportional to the exciton volume. The reason is the different chemical origin of the lowest conduction bands as demonstrated in fig. 3 by the atom-projected density of states. In the Si and Ge cases these bands are dominated by states localized at those atoms. Consequently, strong intra-atomic contributions increase the dipole matrix elements, giving rise to first-class (dipole allowed) excitons. In the carbon case the situation is completely different. Similarly to hydrogenated diamond surfaces, the lowest conduction bands are governed by hydrogen contributions [37]. The first optical transition is dipole forbidden, giving rise to second-class excitons.

For each 2D sheet material the corresponding exciton series in fig. 2 shows a non-monotonous behavior with

respect to both the oscillator strength and the binding energy: the peak positions (and intensities) neither follow the formation law $\sim n^{-2}$ (with intensity $\sim n^{-3}$) for the 3D Wannier-Mott excitons [38], nor the formation law $\sim (n+\frac{1}{2})^{-2}$ (with intensity $\sim (n+\frac{1}{2})^{-3}$) for the 2D Wannier-Mott excitons [39] ($n=1,2,3,\ldots$). Such deviations may be due to the finite thickness, the anisotropy and non-parabolicity of the bands near Γ, and to a screening that cannot be described simply by a dielectric constant. The huge exciton binding energies E_B of the lowest pair excitations, $E_B=1.8$, 0.9, and 0.6 eV (see fig. 2) for C_2H_2, Si_2H_2, and Ge_2H_2, respectively, with their evident chemical trend, are related to the increasing k-dispersion of the bands defining the fundamental gap as well as to the increasing electronic polarizability α_{2D} of the sheets. In the following we illustrate these effects in terms of the peculiar properties of the 2D crystals.

2D excitonic effects: model vs. ab initio calculations. A rough estimate of E_B for the lowest bound pair excitations is possible within a simplified 2D parabolic description of electron and hole motion similar to the situation in a 2D hydrogenic model of the excitons [39]. The bands near Γ in fig. 1 are described within the effective mass approximation. We find average reduced masses $\mu=0.28$ (C_2H_2), 0.09 (Si_2H_2), and $0.05\,m_e$(Ge_2H_2). Their strong variation mainly results from the different effective electron masses $m*_e=1.04$, 0.16, and $0.08\,m_e$. A second ingredient of the simplified exciton picture [39] is the screened Coulomb potential W describing the electron-hole attraction. In the limit of vanishing sheet thickness the 2D Fourier transform of the potential reads as $W(\mathbf{q})=2\pi e^2/\varepsilon(\mathbf{q})|\mathbf{q}|$ with $\varepsilon(\mathbf{q})=1+2\pi\alpha_{2D}|\mathbf{q}|$. The 2D case is fulfilled for sheet thicknesses d and wave vectors $|\mathbf{q}|$ with $d|\mathbf{q}|\to 0$. As a consequence the screening of the electron-hole attraction has to be replaced by its vacuum value for relatively small 2D wave vectors and electron-hole pair distances $r>d$. The 2D electronic polarizability can be estimated by $\alpha_{2D}=L[\epsilon(0)-1]/4\pi$, where $\epsilon(0)$ is the static in-plane electronic dielectric constant of the superlattice system that is used to model the isolated sheets within the *ab initio* calculations, and L is the distance of the repeated sheets. We find $\alpha_{2D}=1.1$, 3.1, and 3.5 Å for the three sheet materials, which almost follows the trend of the static dielectric constants of the bulk group-IV crystals. In real space the screened potential takes the form [40]

$$W(r)=\frac{e^2}{4\alpha_{2D}}\left[H_0(x)-N_0(x)\right]\big|_{x=r/2\pi\alpha_{2D}}, \qquad (1)$$

where $N_0(x)$ and $H_0(x)$ are the Neumann and Struve functions and r is the in-plane radius. In the limit $2\pi\alpha_{2D}\ll r$, eq. (1) reduces to that of a 2D hydrogen atom with $W(r)=-e^2/r$ and hence to a 2D Wannier-Mott problem [39], whereas if $2\pi\alpha_{2D}\gg r$, eq. (1) describes a pronounced sheet exciton whose electron-hole attraction is represented by a logarithmic singularity in the 2D space [40]. It is interesting to notice that, differently from the 3D case, in the 2D hydrogen problem the electron-hole interaction is not screened. This, and the logarithmic behaviour at smaller distances, generates the peculiar trends of 2D excitons seen in fig. 2.

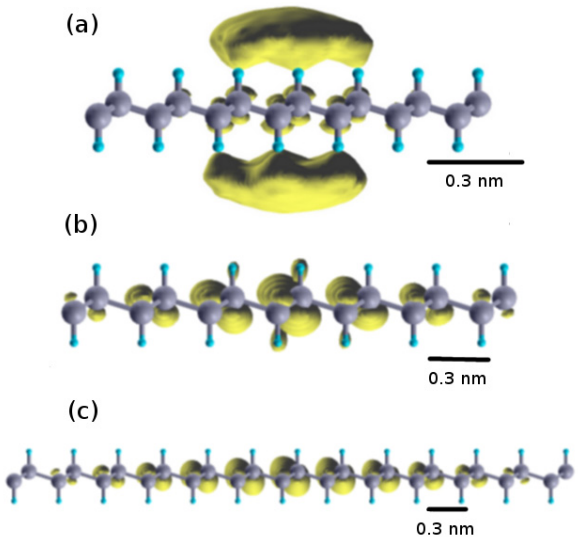

Fig. 4: (Color online) Side view of the lowest-energy exciton wave function in graphane (a), silicane (b), and germanane (c). The hole is assumed to be localized in a σ-bond between two group-IV atoms.

The 2D problem with the screened potential (1) cannot be exactly analytically solved. A variational approach with a $1s$ exciton wave function ($\sim e^{-r/r_{ex}}$) in 2D gives rise to binding energies of about $E_B=2.0$, 0.7, and 0.5 eV in close agreement, both in magnitude and trend, with our *ab initio* values (1.8, 0.9, and 0.6 eV, see fig. 2). The corresponding exciton radii are rather small, especially for graphane, with $r_{ex}=4.3$, 13.0 and 19.8 Å. The order of magnitude of these radii almost matches the one of their *ab initio* counterparts equal to $r_{ex}=5.8$, 9.7, and 16.0 Å, respectively. These values have been derived from the two-particle wave functions illustrated in fig. 4.

The knowledge of E_B and r_{ex} allows a closer characterization of the excitons, *e.g.*, using the dimensionless parameter $\frac{2\pi\alpha_{2D}}{r_{ex}}=1.6$ (C_2H_2), 1.5 (Si_2H_2), and 1.1 (Ge_2H_2). It clearly indicates that none of the two limiting cases $2\pi\alpha_{2D}\ll r_{ex}$ (2D hydrogen-like exciton [39] with an unscreened 2D Coulomb potential (1)) or $2\pi\alpha_{2D}\gg r_{ex}$ (sheet exciton [40] whose electron-hole attraction (1) approaches a potential with a logarithmic singularity in the 2D space) can be used to characterize the excitons. The excitons observed for the three hydrogenated group-IV sheet crystals possess an intermediate character between unscreened Coulomb-like and logarithmic electron-hole attraction modified by the sheet polarization. On the other hand, the almost two-dimensional character of the excitonic excitations is confirmed by the pair wave functions depicted in fig. 4. Important differences in their wave

functions make silicane and germanane quantitatively and qualitatively different from graphane. For graphane (fig. 4(a)) the lateral probability to find the electron for a fixed hole is essentially localized around the nearest-neighbor atoms. The vertical extent is determined by free-electron–like electron states above and below the H atoms. This pair excitation can be identified as a 2D Frenkel exciton. The lateral extent of the probability is much larger for germanane (fig. 4(c)) in agreement with the estimated ($r_{ex} = 19.8$ Å) or *ab initio* computed ($r_{ex} = 16.0$ Å) exciton radius. Therefore, the corresponding pair excitation in germanane shows important features of a 2D Wannier-Mott–like exciton, although the electron-hole attraction is not completely described by a bare Coulomb potential but is modified by the sheet polarizability. Silicane represents an intermediate case but is more similar to germanane than to graphane.

Conclusions. – In conclusion, we have investigated the electronic and optical properties of silicane and germanane by *ab initio* calculations using the many-body perturbation theory, and compared with those of graphane. We observe clear chemical trends due to the size, core and relative electronegativity of the group-IV elements with respect to H. The optical gaps of silicane and germanane are smaller than that of graphane. Excitonic effects are found to be much more important than in the corresponding 3D crystals and non-hydrogenated sheets. As a consequence the optical absorption edge is shifted towards lower photon energies. The emission wavelength even occurs in the visible range. The extremely large binding energies and the large oscillator strengths of the lowest pair excitations in silicane and germanane, together with their 2D character, suggest the observability of interesting physical effects or possible important optoelectronic applications. The vanishing dipole matrix elements in graphane, which give rise to second-class excitons, may allow the observation of an excitonic Bose-Einstein condensate by continuous optical pumping of excitons [10]. In silicane and germanane the giant near-band edge oscillator strengths of first-class excitons, which are by three orders of magnitude larger than in graphane, give rise to extremely short radiative lifetimes preventing condensation and hence a powerful light-matter coupling. However, the combination of large exciton binding energies and large oscillator strengths suggests the occurrence of significant exciton-polariton effects in 2D Si- or Ge-based crystals even at room temperature. Therefore, in contrast to the corresponding 3D materials these sheet crystals should be promising candidates for active optoelectronic devices, *e.g.* light-emitting diodes in the visible or near UV region. Strong excitons in two-dimensional crystals present an enormous interest also from the fundamental point of view as a laboratory for studies of bosonic effects at room temperature, including Bose-Einstein condensation, superfluidity, exciton-mediated superconductivity. Applications may include polariton lasers and optical switches. This work indicates that the new 2D crystals silicane and germanane are extremely promising for the observation of excitonic effects at high temperature and in the visible optical range.

* * *

We acknowledge the CPU time granted by CINECA, ENEA-CRESCO and CASPUR. This work has been supported by the EC (FP7/2007-2013 grants n. 211956 (ETSF), and n.235114 (Clermont4)).

REFERENCES

[1] Katsnelson M. I., *Mater. Today*, **10**, issue No. 1-2 (2007) 20.
[2] Fiori G. *et al.*, *Phys. Rev. B*, **82** (2010) 153404.
[3] Geim A. K., *Science*, **324** (2009) 1530.
[4] Sofo J. O., Chaudhari A. S. and Barber G. D., *Phys. Rev. B*, **75** (2007) 153401.
[5] Ryu S. *et al.*, *Nanoletters*, **8** (2008) 4597.
[6] Elias D. C. *et al.*, *Science*, **323** (2009) 610.
[7] Lebégue S. *et al.*, *Phys. Rev. B*, **79** (2009) 245117.
[8] Pulci O. *et al.*, *Phys. Status Solidi (a)*, **207** (2010) 291.
[9] Marsili M. and Pulci O., *J. Phys. D*, **43** (2010) 374016.
[10] Cudazzo P. *et al.*, *Phys. Rev. Lett.*, **104** (2010) 226804.
[11] Samarakoon D. K. *et al.*, *Small*, **7** (2011) 965.
[12] Guzmán-Verri G. G. and Lew Yan Voon L. C., *Phys. Rev. B*, **76** (2007) 075131.
[13] Cahangirov S. *et al.*, *Phys. Rev. Lett.*, **102** (2009) 236804.
[14] Lebégue S. and Eriksson O., *Phys. Rev. B*, **79** (2009) 115409.
[15] Sheka E. F., arXiv:0901.3663 (2009).
[16] Sahin H. *et al.*, *Phys. Rev. B*, **80** (2009) 155453.
[17] De Padova P. *et al.*, *Appl. Phys. Lett.*, **96** (2010) 261905.
[18] Nakano H. *et al.*, *Angew. Chem.*, **118** (2006) 6451.
[19] Dahn J. R. *et al.*, *Phys. Rev. B*, **48** (1993) 17872.
[20] Vogg G., Brandt M. S. and Stutzmann M., *Adv. Mater.*, **12** (2000) 1278.
[21] Van de Walle C. G. and Northrup J. E., *Phys. Rev. Lett.*, **70** (1993) 1116.
[22] Lew Yan Voon L. C. *et al.*, *Appl. Phys. Lett.*, **97** (2010) 163114.
[23] Garcia J. C., de Lima D. B., Assali L. V. C. and Justo J. F., *J. Phys. Chem. C*, **115** (2011) 13242.
[24] Houssa M., Scalise E., Sankaran K., Pourtois G., Afanas'ev V. V. and Stesmans A., *Appl. Phys. Lett.*, **98** (2011) 223107.
[25] Miller R. D. and Michl J., *Chem. Rev.*, **89** (1989) 1359.
[26] Miller R. D. and Sooriyakumaran R., *J. Polym. Sci. Part A: Polym. Chem.*, **25** (1987) 111.
[27] Takeda K., *J. Phys. Soc. Jpn.*, **63**, Suppl. B (1994) 1.
[28] Giannozzi P. *et al.*, *J. Phys.: Condens. Matter*, **21** (2009) 395502.
[29] Hedin L. and Lundquist B. J., in *Solid State Physics*, edited by Ehrereich H., Seitz F. and Turnbull D., Vol. **23** (Academic Press, New York) 1969, p. 1.
[30] GW calculations have been performed at the level of the G_0W_0 approximation, using $50 \times 50 \times 1$ k-points for

the screen and a plasmon pole approximation. For the exchange part of the self-energy, $90 \times 90 \times 1$ k-points have been used. The Coulomb potential has been cut in the z-direction. In the BSE, $50 \times 50 \times 1$ k-points, four valence bands and five empty bands have been included. Exc code: `http://etsf.polytechnique.fr/exc/`.

[31] Onida G., Reining L. and Rubio A., *Rev. Mod. Phys.*, **74** (2002) 601.

[32] Hajnal Z. *et al.*, *Phys. Rev. B*, **64** (2001) 033311.

[33] Alzahrani A. Z. and Srivastava G. P., *Appl. Surf. Sci.*, **256** (2010) 5783.

[34] Hirayama M. *et al.*, *J. Surf. Sci. Nanotechnol.*, **4** (2006) 528.

[35] Nakano H. *et al.*, *J. Am. Ceram. Soc.*, **88** (2005) 3522.

[36] Dettlaff-Weglikowska U. *et al.*, *Phys. Rev. B*, **56** (1997) 13132.

[37] Bechstedt F. *et al.*, *Phys. Rev. Lett.*, **87** (2001) 016103.

[38] Elliott R. J., *Phys. Rev.*, **108** (1957) 1384.

[39] Shinada M. and Sugano S., *J. Phys. Soc. Jpn.*, **21** (1966) 1936.

[40] Keldysh L. V., *Pisma Zh. Eksp. Theor. Fiz.*, **29** (1979) 716; *JETP Lett.* **29** (1979) 658.